

1 **Cadmium and phosphate in coastal Antarctic**
2 **seawater: implications for Southern Ocean nutrient**
3 **cycling**

4
5 *Katharine R Hendry*¹

6
7 *Rosalind E M Rickaby*¹

8
9 *Jan C M de Hoog*¹

10
11 *Keith Weston*²

12
13 *Mark Rehkämper*³

14
15 ¹Department of Earth Sciences, University of Oxford, Parks Road, Oxford, OX1 3PR,
16 UK

17 ²Laboratory for Global Marine and Atmospheric Chemistry, School of Environmental
18 Sciences, University of East Anglia, Norwich, NR4 7TJ, UK

19 ³Department of Earth Sciences and Engineering, Imperial College, University of
20 London, South Kensington, London, SW7 2AZ, UK

21

22

23 **1 Abstract**

24 Cadmium is a biologically important trace metal that co-varies with phosphate (PO_4^{3-})
25 or Dissolved Inorganic Phosphate, DIP) in seawater. However, the exact nature of Cd
26 uptake mechanisms and the relationship with phosphate and other nutrients in global
27 oceans remains elusive. Here, we present a time series study of Cd and PO_4^{3-} from
28 coastal Antarctic seawater, showing that Cd co-varies with macronutrients during
29 times of high biological activity even under nutrient and trace metal replete
30 conditions. Our data imply that $\text{Cd}/\text{PO}_4^{3-}$ in coastal surface Antarctic seawater is
31 higher than open ocean areas. Furthermore, the sinking of some proportion of this
32 high $\text{Cd}/\text{PO}_4^{3-}$ water into Antarctic Bottom Water, followed by mixing into
33 Circumpolar Deep Water, impacts Southern Ocean preformed nutrient and trace metal
34 composition. A simple model of endmember water mass mixing with a particle
35 fractionation of Cd/P ($\alpha_{\text{Cd-P}}$) determined by the local environment can be used to
36 account for the $\text{Cd}/\text{PO}_4^{3-}$ relationship in different parts of the ocean. The high
37 $\text{Cd}/\text{PO}_4^{3-}$ of the coastal water is a consequence of two factors: the high input from
38 terrestrial and continental shelf sediments and changes in biological fractionation with
39 respect to P during uptake of Cd in regions of high Fe and Zn. This implies that the
40 $\text{Cd}/\text{PO}_4^{3-}$ ratio of the Southern Ocean will vary on glacial-interglacial timescales as
41 the proportion of deep water originating on the continental shelves of the Weddell Sea
42 is reduced during glaciations because the ice shelf is pinned at the edge of the
43 continental shelf. There could also be variations in biological fractionation of Cd/P in
44 the surface waters of the Southern Ocean on these timescales as a result of changes in
45 atmospheric inputs of trace metals. Further variations in the relationship between Cd
46 and PO_4^{3-} in seawater arise from changes in population structure and community
47 requirements for macro- and micronutrients.

48

49 Keywords: cadmium, phosphate, coastal, nutrients, Southern Ocean

50 **2 Introduction**

51 Major nutrients (macronutrients) carbon (C), nitrate (NO_3^-), phosphate (PO_4^{3-}) and, in
52 the case of siliceous organisms, silicic acid (Si or $\text{Si}(\text{OH})_4$), are taken up into the
53 organic and skeletal material of marine phytoplankton in the euphotic zone,
54 repackaged by zooplankton and exported as dead cells and fecal pellets. Over 86% of
55 the carbon flux at 100 m is remineralised by 1000 m depth, such that macronutrients
56 exhibit characteristic vertical gradients (Martin et al., 1987). In addition to these
57 macronutrients, trace amounts of other elements (micronutrients) are essential for
58 phytoplankton growth. Although studies into micronutrient biogeochemical cycling
59 have focused on Fe availability, other metals, such as Cd, may be biologically
60 important. Cd is a labile nutrient associated with organic matter and has similar
61 spatial distribution patterns to PO_4^{3-} in open ocean deep and surface waters (Boyle,
62 1988; Figure 1). The exact nature of the relationship between Cd and P has been
63 discussed extensively in the literature, and has been modelled either as a combination
64 of two linear relationships separated by a “kink” at $\sim 1.3 \mu\text{mol kg}^{-1} \text{PO}_4^{3-}$ as a result of
65 basin specific processes (Cullen, 2006; de Baar et al, 1994; Frew and Hunter, 1992;
66 Yeats, 1998) or a non-linear fractionation curve (Elderfield and Rickaby, 2000).

67 There is increasing evidence that Cd is a biologically important trace metal, actively
68 taken up by phytoplankton in productive surface waters. Firstly, Cd is known to
69 substitute into the metalloenzyme Carbonic Anhydrase (CA), which catalyses the
70 uptake of bicarbonate (HCO_3^-) from seawater providing a source of inorganic C for
71 photosynthesis i.e. the Carbon Concentrating Mechanism or CCM (Morel and Price,

72 2003). Cd may substitute for Zn in CA such that Cd added to Zn-limited diatoms
73 leads to an increase in cellular CA activity and growth rate (Lane and Morel, 2000;
74 Lee and Morel, 1995; Morel et al., 1994; Price and Morel, 1990). Recent sequencing
75 and primary characterisation has confirmed the presence of a Cd specific CA, i.e. Cd-
76 CA; (Lane et al., 2005; Xu et al., 2008). Cd has also been implicated in the formation
77 of Polyphosphate Bodies (PPBs) in the giant kelp, *Macrocystis pyrifera*. PPBs are
78 ubiquitous to most organisms, and may be active in phytoplankton (Hunter and Boyd,
79 1997). Secondly, recent seawater analyses have shown that Cd isotopic fractionation
80 occurs in seawater, with the greatest fractionation occurring in surface waters depleted
81 in dissolved Cd suggesting a biological signature (Lacan et al., 2006; Ripperger et al.,
82 2007).

83 Biological uptake, and thus changes in nutrient demands due to variations in
84 environmental conditions and population structure, could have a significant impact on
85 the relationship between Cd and P in seawater. In addition to providing insight into
86 modern biogeochemical cycling, understanding the relationship between macro- and
87 micronutrients has implications for the reconstruction of past PO_4^{3-} utilisation using
88 Cd/Ca ratios in foraminiferal calcite, which relies on a predictable Cd/ PO_4^{3-} ratio in
89 seawater (Boyle, 1986; Rickaby & Elderfield, 1999; Elderfield & Rickaby, 2000).
90 The chemistry of deep water masses could be influenced by continental shelf and
91 coastal processes at the site of formation. Further, past changes in continental shelf
92 inputs to deep water could impact past deep water Cd/ PO_4^{3-} , and, consequently, the
93 interpretation of benthic foraminiferal Cd/Ca ratios. Here, we investigate the seasonal
94 uptake of Cd and macronutrients in a coastal environment off the West Antarctic
95 Peninsula. We discuss our results in the context of Southern Ocean processes on a

96 wider spatial scale, and the implications of our results for seawater Cd/PO₄³⁻ over
97 longer timescales.

98

99 **3 Methods and materials**

100 ***3.1 Field setting***

101 Coastal seawater samples were collected from Ryder Bay, which forms the larger part
102 of Marguerite Bay off Adelaide Island, near Rothera Research Station (British
103 Antarctic Survey, BAS), West Antarctic Peninsula (WAP; Figure 2). As well as
104 being ideally located in a climatically sensitive region (Meredith et al., 2004), this site
105 is part of several long term monitoring projects (Clarke et al., 2008; Meredith et al.,
106 2008; Smith et al., 1999). The Rothera Oceanographic and Biological Time-Series
107 (RaTS) has been conducted by BAS since late 1997, following the end of the
108 successful long term monitoring series at Signy, northern WAP, in 1994.
109 Conductivity-Temperature-Depth (CTD) profiles, nutrient analysis and size
110 fractionated pigment assays (to monitor biomass) are carried out on a regular basis
111 throughout the year and further details are reported elsewhere (Clarke et al., 2008).

112

113 The Antarctic Circumpolar Current (ACC) pumps nutrient rich, oxygen poor, warm
114 water from the Upper Circumpolar Deep Water (UCDW) onto the continental shelf
115 along the WAP below 200 m and into Marguerite Bay several times a year (Meredith
116 et al., 2004). Vertical mixing of this water occurs largely as a result of bathymetric
117 features and is the principal heat transfer process at depth. Above 100-150 m, the
118 highly seasonal Antarctic Surface Water (ASW) dominates in shelf waters, including
119 Marguerite Bay. In the summer months, the surface water is separated from deeper

120 water by a strong pycnocline, which develops as a result of warming and freshening
121 and can be defined by a Mixed Layer Depth (MLD). This pycnocline isolates a
122 remnant of the water column, which is well mixed in winter, termed the Winter Water
123 Mass (WW) (Clarke et al., 2008; Meredith et al., 2008; Meredith et al., 2004).

124

125 ***3.2 Field methods***

126 Water column samples were collected 2-3 times a week from January to March in
127 2005 and 2006 at the RaTS site (Figure 2). The samples were collected from 15 m,
128 the average chlorophyll maximum in Ryder Bay (Clarke et al., 2008), filtered using
129 0.2 µm polycarbonate membranes (Whatman), acidified to pH 1.7-1.9 using sub-
130 boiling quartz distilled HNO₃ under trace metal clean conditions and stored at 4°C.
131 All plasticware used during collection, filtration and analysis was acid-cleaned by
132 soaking in 1 N HNO₃ (AnalaR) for at least 24 hours and rinsing thoroughly in 18 MΩ
133 cm Milli-Q water. Laboratory blanks of 18 MΩ cm Milli-Q water were run through
134 the complete protocol outlined to test for contamination in the laboratory.

135 Additional samples were filtered for silicic acid and phosphate analysis. Glass fibre
136 filters (Whatman GF/F; nominal pore size 0.8µm) are routinely used to filter seawater
137 for N and P analysis. Silica free polycarbonate 0.2 µm filter membranes (Whatman)
138 were used to filter seawater for silicic acid (Si) analysis to avoid contamination by any
139 Si released from the glass fibres of the GF/F membranes. Samples for NO₃⁻ and PO₄³⁻
140 analysis were stored at -20°C; samples for silicic acid analysis were stored at 4°C.

141 ***3.3 Laboratory methods***

142 *i) Initial Cd determinations by standard addition*

143 Approximate trace metal concentrations were measured on a Perkin Elmer Elan
144 6100DRC Quadrupole Inductively Coupled Plasma Mass Spectrometer (Q-ICP-MS)
145 using a standard addition method. Five aliquots of acidified seawater were diluted
146 ten-fold with 1% sub-boiling quartz-distilled HNO₃ and added to incremental amounts
147 of spike solutions (Greyhound Chromatography). A machine blank was initially run
148 for each batch of five solutions. Pulse intensity was measured six times for each
149 aliquot, the mean value corrected for isobaric interferences and machine blank, and
150 sample concentration calculated by regression.

151 Cd intensities were measured using ¹¹⁴Cd (28.73% natural Cd). Isobaric interference
152 from ¹¹⁴Sn (0.65% natural Sn) was corrected for by measuring ¹¹⁸Sn, and ⁹⁸Mo¹⁶O⁺
153 was corrected for by monitoring ⁹⁸Mo intensities. ⁹⁸Mo¹⁶O⁺/⁹⁸Mo⁺ formation in the
154 plasma is 0.2 to 0.4%. The external precision and accuracy were assessed using two
155 independent seawater standards (Table 1). These approximate concentrations were
156 used to determine the optimal quantities of Cd spike that were to be added to the
157 samples, to avoid large error magnification factors in the application of the isotope
158 dilution method. Laboratory blanks were also measured by standard addition, and
159 were below the Limit of Detection (LoD for Cd ~ 0.01 ppb).

160

161 *ii) Isotope dilution method*

162 The small variations in Cd concentrations during the 2006 austral summer were
163 subsequently measured by single-spike isotope dilution after pre-concentration of Cd
164 by Mg(OH)₂ co-precipitation (Wu and Boyle, 1997). An appropriate amount of spike,
165 which had been previously calibrated (Ripperger and Rehkämper, 2007a; Ripperger
166 and Rehkämper, 2007b), was weighed into Teflon containers. Error magnification
167 was reduced by keeping the sample-to-spike mass ratio for Cd approximately equal to

168 unity. As the co-precipitation method is pH sensitive, the concentration and acidity of
169 the spike were adjusted after weighing. Approximately 13 ml of acidified seawater
170 was weighed in 15 ml acid-cleaned polypropylene centrifuge tubes (5 point balance \pm
171 0.01 mg) and spiked with 400 μ l of enriched ^{110}Cd spike solution was added.
172 Previous experiments have shown that the equilibration is rapid, and there is no
173 significant difference between samples equilibrated for 2 minutes and 2 days (Wu and
174 Boyle, 1997). FEP distilled aqueous NH_3 (500-2000 μ l) was added to precipitate
175 $\text{Mg}(\text{OH})_2$; the amount added was determined empirically to allow $\sim 7\%$ Mg to
176 precipitate to minimise matrix effects during analysis (Mg ~ 1000 ppm; (Wu and
177 Boyle, 1997)). Cd is preferentially taken up into the precipitate, resulting in $\sim 30\%$
178 Cd yields. After NH_4OH addition, the sample was left for two minutes before
179 centrifugation at 6000 rpm for 4 minutes. The supernatant was discarded and the
180 precipitate was redissolved in 0.5 ml 5% HNO_3 (sub-boiling distilled HNO_3 in Milli-
181 Q water), diluted with 0.5 ml Milli-Q and analysed for Cd isotopes by ICP-MS.
182 The standards and samples were analysed using an Element II magnetic sector ICP-
183 MS (Thermo Finnigan), introduced in conjunction with a Cetac ASX-100
184 microautosampler. The ICP-MS was run in low resolution mode to optimise counting
185 statistics; using medium resolution reduces the signal by a factor of 15. Even though
186 $\text{Mg}(\text{OH})_2$ co-precipitation significantly lowers the matrix load of the seawater
187 samples, elements that potentially interfere with Cd isotopes, such as Mo, Sn and Pt,
188 are precipitated along with Cd and need to be monitored. Standards were measured
189 for mass bias and oxide corrections. Two standard solutions were used: 1) a 1 ppb
190 “Alfa Cd Zürich” Cd standard (Ripperger and Rehkämper, 2007b), the isotopic
191 composition of which is known accurately and precisely and is very similar to that of
192 the bulk silicate Earth (Table 2); 2) “Ryder06”, an in-house standard of seawater from

193 Ryder Bay that has undergone the sample preparation procedures, and therefore
194 represents an unspiked version of the samples.

195 Each sample was bracketed with a blank, and the “Alfa Cd Zürich” Cd standard was
196 run every 3 samples. The standard “Ryder06” was spiked with various amounts of In,
197 Mo and Cd to obtain signal corrections within a matrix similar to that of the samples
198 (see below for details). It was also measured at the beginning of each run without any
199 additives to test the validity of the blank and oxide corrections on the Cd signals
200 discussed below.

201 The ion beam intensities of ^{110}Cd , ^{111}Cd , ^{112}Cd , ^{114}Cd were measured and ^{106}Pd , ^{95}Mo ,
202 ^{98}Mo and ^{118}Sn were monitored for interference corrections. Analytical conditions are
203 listed in Table 3. An extended E-Scan range of 30% was used, which allowed rapid
204 scanning without magnet jumps, hence a more efficient duty cycle and better
205 precision. The tuning of the instrument was optimised for maximum Cd intensity and
206 low oxide formation rates. Molybdenum oxides provided the most significant
207 polyatomic interferences (Table 4), with $^{98}\text{Mo}^{16}\text{O}^+ / ^{98}\text{Mo}^+$ values of 0.07-0.10%.
208 Further corrections were made by assessing the interferences on standards before the
209 samples were measured. A solution of “Ryder06” that had been spiked with 10 ppm
210 Mo was measured prior to each run to assess MoO^+ formation. A pure Mo standard
211 was measured before each run to determine mass bias corrections for MoO
212 compounds that were not measured in the actual sample run (such as $^{94}\text{MoO}^+$ and
213 $^{96}\text{MoO}^+$); these interferences were then corrected using either ^{95}Mo or ^{98}Mo count
214 rates. ^{114}Cd and ^{112}Cd were corrected for ^{114}Sn and ^{112}Sn by measuring ^{118}Sn and using
215 the natural $^{114}\text{Sn}/^{118}\text{Sn}$ and $^{112}\text{Sn}/^{118}\text{Sn}$ ratios, respectively.

216 ^{110}Pd interference on ^{110}Cd was corrected by monitoring ^{106}Pd after Mo and Sn
 217 corrections, and after correcting ^{106}Pd for ^{106}Cd based on ^{111}Cd signals as follows
 218 (Equations 1-2):

$$219 \quad {}^{110}\text{Cd}_{\text{corr}} = {}^{110}\text{Cd}^* - {}^{106}\text{Pd}_{\text{corr}} / A_{106\text{Pd}} \times A_{110\text{Pd}} \quad (1)$$

$$220 \quad {}^{106}\text{Pd}_{\text{corr}} = {}^{106}\text{Cd}^* - {}^{111}\text{Cd}^* / A_{111\text{Cd}} \times A_{106\text{Cd}} \quad (2)$$

221 where A_x = natural abundance of isotope, and the superscript * denotes count rates
 222 corrected for blank and MoO contributions.

223

224 The strong matrix effect of the sample solutions (about 1000 ppm each of Mg and Na)
 225 obtained by co-precipitation samples results in a suppression of the instrument blank
 226 signal. This suppression, and so the true instrument blank, was assessed by measuring
 227 the intensity of an In spike added to both 2% HNO_3 and the in-house standard
 228 ‘Ryder06’ standard and then applying Equation 3:

$$229 \quad B = \frac{In_{\text{Ryder06}}}{In_{2\%}} \times B_{2\%} \quad (3)$$

230 where In_{Ryder06} = In intensity in Ryder06

231 $In_{2\%}$ = In intensity in 2% acid

232 $B_{2\%}$ = Machine blank for 2% acid

233

234 Blank contributions were about 5% of the signal for all Cd isotopes except ^{112}Cd ca.
 235 40%. Mass bias (Δ_M) was corrected by measuring the isotope ratio of a 1 ppb solution
 236 of “Alfa Cd Zürich” and applying Equation 4:

237

$$\Delta_M = \frac{\left[\frac{{}^{110}\text{Cd}}{{}^{111}\text{Cd}} \right]_{\text{measured}}}{\left[\frac{{}^{110}\text{Cd}}{{}^{111}\text{Cd}} \right]_{\text{real}}} - 1 \quad (4)$$

239

240 The natural sample ratio (or the ratio of the in-house Ryder06 standard) may not be
 241 exactly equal to the ratio of the Alfa Cd Zürich standard. Natural Cd isotopic
 242 fractionation in seawater occurs as a result of closed system biological uptake and
 243 ranges from $\epsilon^{114/110} \text{Cd} = \pm 3$ to ± 36 (Ripperger et al., 2007). However, the greatest
 244 fractionations occurs in Cd-depleted surface waters in the North Pacific ($[\text{Cd}] \sim 0.003$
 245 nmol kg^{-1}). The $[\text{Cd}]$ concentration of the Ryder Bay surface waters are higher,
 246 suggesting a lower degree of Cd isotopic fractionation, and are replenished regularly
 247 by deep water ($\epsilon^{114/110} \text{Cd} = \pm 3.3 \pm 0.5$; (Ripperger et al., 2007)). Hence, the
 248 maximum error associated with assuming $\epsilon^{114/110} \text{Cd} = 0$ is approximately 0.03%.

249

250 The external reproducibility of the isotope analysis was established by repeat
 251 measurements of unspiked standard “Ryder06”, and was found to be approximately
 252 2% (Figure 3). The reproducibility for spiked samples should be as good as or better
 253 than 2% due to the greater proportion of ${}^{110}\text{Cd}$. The accuracy of the isotope dilution
 254 method was determined based on duplicate measurements of the reference standard
 255 NASS-5, which yielded concentrations of 0.0221 ± 0.0004 (~2%) and 0.021 ± 0.006
 256 (~30%) ppb using ${}^{110}\text{Cd}/{}^{114}\text{Cd}$ and ${}^{110}\text{Cd}/{}^{111}\text{Cd}$ respectively (certified value $0.023 \pm$
 257 0.003 ; measured as 0.02224 ± 0.00004 by double spiked isotope dilution, (Ripperger
 258 and Rehkämper, 2007b)). ${}^{110}\text{Cd}/{}^{114}\text{Cd}$ and ${}^{110}\text{Cd}/{}^{111}\text{Cd}$ agree well for the samples
 259 (Figure 4), but due to the greater precision on the former ratio, only concentrations
 260 determined via ${}^{110}\text{Cd}/{}^{114}\text{Cd}$ ratios are quoted in the results section.

261

262 Macronutrients were measured using a Skalar Autoanalyser (Kirkwood, 1996). The
263 detection limit for NO_3^- , PO_4^{3-} and Si analyses were 0.1, 0.05 and 0.1 $\mu\text{mol l}^{-1}$
264 respectively. The percentage error for all nutrient analyses was less than 5% relative
265 to Ocean Scientific International (U.K.) standards. This results in a propagated error
266 of $\sim 5.5\%$ on $\text{Cd}/\text{PO}_4^{3-}$ values.

267

268 **4 Results and discussion**

269

270 Our time series shows a consistent pattern of biological utilisation, with seasonal
271 depletion in macronutrients NO_3^- and PO_4^{3-} during periods of high biomass (Figure 5).
272 Cd co-varies with macronutrients (using all available data, Cd versus PO_4^{3-} , $r^2 = 0.70$,
273 $n = 18$) with depletions occurring during the peaks of the summer bloom. However,
274 the relationship between total chlorophyll *a* (chl *a*) and both macronutrients and Cd is
275 not statistically significant ($r^2 < 0.1$ for chl *a* versus $\text{Si}(\text{OH})_4$, PO_4^{3-} , NO_3^- and Cd).
276 This suggests that chl *a*, a measure of biomass, may not in this situation provide a
277 reliable measure of nutrient utilisation *per se*. This could be because 1)
278 phytoplankton utilise a range pigments in addition to chl *a*; 2) biomass does not relate
279 to total nutrient drawdown because of grazing and remineralisation processes; 3)
280 abiological/physical factors, such as storminess and water column mixing, influence
281 the distribution of nutrients (Clarke et al., 2008).

282

283 **4.1 Comparison between open ocean and coastal Cd/ PO₄³⁻:**

284 ***implications for Southern Ocean chemistry***

285 The “global relationship” between Cd and P reflects various interactions between
286 mixing of water masses containing different preformed nutrients and surface water
287 biological fractionation. The non-linear nature of the relationship is not fully
288 understood and may be a result of several different mechanisms (Cullen, 2006). The
289 new Cd and PO₄³⁻ data from Ryder Bay presented here (Figure 5, 6) are consistent
290 with other published coastal datasets and appear offset towards higher Cd/P compared
291 to the global open ocean trend (Frew, 1995; Jones and Murray, 1984; Van Geen and
292 Luoma, 1993). Here, we suggest the Cd/PO₄³⁻ of a parcel of surface seawater is
293 determined by the initial Cd/PO₄³⁻, set by inputs from upwelling and terrestrial runoff,
294 and the subsequent fractionation trajectory of biological utilisation. The initial offset
295 towards higher Cd values in coastal regions is a result of input from continentally
296 derived sediments and the high Cd/PO₄³⁻ composition of upwelling water. The
297 biological utilisation trajectory in these coastal regions follows a curve with reduced
298 uptake of Cd with respect to PO₄³⁻ compared to open ocean regions (Figure 6).
299 Variability in the extent of such enrichment in Cd over that expected for a given PO₄³⁻
300 concentration is most likely to relate to spatial variation in the micronutrient content
301 of the water column due to variations in upwelling, phytoplankton nutrient
302 requirements and community structure.

303 **4.1.1 Initial Cd/ PO₄³⁻ of upwelling water: continental input and water**

304 **mass mixing**

305 The most likely sources of high Cd/P inputs to our coastal setting are continental shelf
306 sediments and terrestrial runoff from glaciers. Coastal and Continental Shelf Waters

307 (CCSW) contain higher Fe and Al inputs as a result of shelf sediment remineralisation
308 and terrestrial input (Measures, pers. com.). In contrast to Fe and Al, Cd precipitates
309 from porewaters and becomes concentrated in reducing sediments (Gobeil et al.,
310 1997). However, in oxic layers at the sediment-water interface, the decomposition of
311 organic matter can release Cd, which is largely mobile (Nolting et al., 1999). The
312 surface layers of Antarctic continental sediments are generally organic rich and
313 oxygenated, and these sediments, possibly with direct input from glacial runoff, will
314 be a significant source of Cd to seawater.

315

316 We can assess the influence of these high Cd/PO₄³⁻ coastal waters on the deep waters
317 that emanate from the Weddell Sea using a mixing model of endmember water
318 masses. Antarctic Bottom Water (AABW) forms largely on the Antarctic continental
319 shelf and shows a correspondingly high Cd/PO₄³⁻ value. The upwelling of
320 Circumpolar Deep Water (CDW), formed from a mixture of aged North Atlantic Deep
321 Water (NADW) and AABW, can be observed in measurements of Cd and PO₄³⁻
322 measurements from open ocean regions of the Southern Ocean (Figure 6). We can
323 use a simple mass balance calculation to quantify the impact of shelf water on CDW.
324 Assuming endmember compositions of NADW and CCSW have [Cd] of 0.3 and 0.8
325 nM and PO₄³⁻ of 1.6 and 2.3 μM respectively (from Figure 6), Modern CDW can be
326 explained by entrainment of shelf waters in a mixing ratio of 40:60 NADW:CCSW
327 (Figure 6). This mixing ratio is also supported by the oxygen isotope signature of
328 AABW and Weddell Sea waters (Frew et al., 1995) and a simple mass balance
329 calculation based on salinity. Assuming NADW and CCSW have salinities of 34.9
330 and 34.6 psu respectively (Adkins et al., 2002; Clarke et al., 2008; Meredith et al.,

331 2008), then a 40:60 ratio of NADW:CCSW explains the Modern CDW salinity of
 332 34.7 psu.

333 4.1.2 Biological fractionation

334 The subsequent biological fractionation of the mixed water upwelling to the surface in
 335 the Southern Ocean will depend on environmental conditions. In open ocean regions
 336 the fractionation of Cd with respect to P follows a simple fractionation trend given by
 337 Equation 6, where Cd_T and P_T are the total Cd and P available in the ocean, Cd_{sw} and
 338 P_{sw} is the concentration of Cd and P in seawater, and α_{Cd-P} is the fractionation factor as
 339 defined in Equation 5 (Elderfield and Rickaby, 2000).

340

$$341 \alpha_{Cd-P} = \frac{\left(\frac{Cd}{P}\right)_{organic}}{\left(\frac{Cd}{PO_4^{3-}}\right)_{seawater}}$$

342 (5)

$$343 Cd_{sw} = Cd_T / \left\{ \alpha_{Cd-P} \left(\frac{P_T}{PO_4^{3-}_{sw}} - 1 \right) + 1 \right\}$$

344

(6)

345 In the CCSZ (e.g. this study and the Princess Elizabeth Trough, (Frew, 1995)), the
 346 relative requirements of Cd with respect to PO_4^{3-} are diminished, α_{Cd-P} is reduced
 347 (Equation 7) and there is a stock of Cd that is not appear to be utilised (“ Cd_{xs} ”).

$$348 Cd_{sw} = (Cd_T - Cd_{xs}) / \left\{ \alpha_{Cd-P} \left(\frac{P_T}{PO_4^{3-}_{sw}} - 1 \right) + 1 \right\} + Cd_{xs}$$

349

(7)

350

351

352 This reduction in relative Cd requirements in coastal regions with respect to the open
353 ocean may be due to differences in the activity of metalloenzymes, such as CA. The
354 activity of CA is affected by the availability of macronutrients (Wang and Dei, 2001),
355 micronutrients (Cullen et al., 2003; Cullen and Sherrell, 2005; Sunda and Huntsman,
356 1998) and pCO₂ (Cullen and Sherrell, 2005). Coastal regions show depleted seawater
357 CO₂ in summer compared to the open Southern Ocean, suggesting variations in pCO₂
358 cannot provide a mechanism to explain the observed seawater Cd/PO₄³⁻ (Álvarez et
359 al., 2002; Bakker et al., 1997; Gibson and Trull, 1999; Hoppema et al., 2000;
360 Takahashi et al., 2002). Hence, the most likely explanation for the lower utilisation of
361 Cd is that the higher micronutrient conditions in coastal waters influences CA activity,
362 Cd requirements or uptake mechanisms. It has been postulated that the non-linear
363 relationship between Cd and PO₄³⁻ is a result of two different fractionation
364 relationships between Cd and PO₄³⁻ in Fe replete and deficient conditions (Cullen et
365 al., 2003). Under high Fe conditions, Cd/P uptake into cellular material is reduced,
366 possibly due to a competing Fe-Cd cellular transporter (Armbrust, 2004; Cullen,
367 2006). Furthermore, the substitution of Zn into the Cd-CA structure influences the
368 enzyme activity, such that CA activity and Cd requirements vary with Zn
369 concentrations in the ambient medium (Park et al., 2007; Xu et al., 2008).

370

371 In Fe and Zn deficient regions (e.g. Subantarctic Zone), uptake of Cd with respect to P
372 follows a simple trend given by Equation 6 with a constant fractionation factor, α_{Cd-P}
373 = 3.5. In Fe and Zn replete conditions of the CCSZ (e.g. Table 5) uptake of Cd
374 follows a trend with a lower fractionation factor ($\alpha_{Cd-P} = 2$; Figure 6). Phytoplankton
375 grown under such conditions have lower Cd requirements (Cullen, 2006), which could

376 provide a mechanism behind the lower value of $\alpha_{\text{Cd-P}}$ in coastal waters. Further,
377 competitive interaction between metals (Sunda and Huntsman, 1998) or biologically
378 produced ligands (Lee et al., 1996) can modulate uptake of Cd. For example,
379 production of metal-binding polypeptides, phytochelatins, is activated in cultured
380 diatoms under high internal and external Cd concentrations (Lee et al., 1996).
381 Increased production of phytochelatins under higher micronutrient conditions could
382 explain the reduction in uptake of Cd in coastal zones.

383

384 ***4.2 Seasonal variability and population structure***

385

386 Our data show some scatter about the linear relationship between Cd and PO_4^{3-} in
387 Ryder Bay (Figure 6), which reflects seasonal variations in seawater $\text{Cd}/\text{PO}_4^{3-}$ due to
388 changes in diatom species composition and environmental conditions. Such
389 population related variations may also influence large scale global cycling of macro-
390 and micronutrients in seawater given the predictable geographical variation in
391 plankton types and sizes.

392

393 Surface $\text{Cd}/\text{PO}_4^{3-}$ of Ryder Bay has an initial background of $\sim 0.4\text{-}0.5 \text{ nmol}/\mu\text{mol}$
394 (Figure 5). Although this estimate is based on approximate concentrations measured
395 using standard addition, it agrees well with other Antarctic coastal regions, e.g.
396 Deception Island ~ 0.6 ; Palmer Station $0.3\text{-}0.35$; (Sañudo-Wilhelmy et al., 2002).
397 These values are also similar to the upper estimates of $\text{Cd}/\text{PO}_4^{3-}$ for UCDW, $0.35\text{-}0.5$
398 $\text{nmol}/\mu\text{mol}$ (Löscher et al., 1998). This is consistent with coastal Antarctic seawater
399 being influenced by high $\text{Cd}/\text{PO}_4^{3-}$ waters from upwelling UCDW (Meredith et al.,
400 2004).

401

402 During the first bloom (Jan-Feb 2006), the Cd/PO₄³⁻ ratio in seawater increases as the
403 uptake of P increases proportionately more than Cd with growth rate. As the early
404 bloom declines, both Cd and P are remineralised and replaced by upwelling water
405 restoring the Cd/PO₄³⁻ to near background levels. Growth rates increase again during
406 the late bloom (Feb-Mar), resulting in an increase in Cd/PO₄³⁻.

407 Cd requirements are lower with respect to PO₄³⁻ (i.e. Cd/PO₄³⁻ is higher) for the late
408 bloom than for the early bloom, which may reflect differences in community structure
409 or environmental conditions, such as changes in photoperiod and temperature.
410 Macro- and micronutrient requirements are a function of cell size (e.g. Ho et al.,
411 2003) and, in particular, it is thought that smaller plankton have lower Cd uptake rates
412 (Finkel et al., 2007) and greater PO₄³⁻ requirements and uptake efficiencies (Asknes
413 and Egge, 1991; Gligora et al., 2007; Wen et al., 1997). Indeed, in Ryder Bay, there
414 is a greater contribution to surface productivity by smaller pico- and nanoplankton (<
415 20 µm) with respect to microplankton (> 20 µm) during the late summer bloom
416 corresponding with higher Cd/PO₄³⁻ (Figure 5). In addition to size, a shift in
417 dominant phytoplankton community can also result in a shift in bulk community Cd
418 requirements. Further, these requirements can change with environmental conditions
419 to varying extents with different divisions. For example, laboratory cultures of
420 diatoms show an increase in Cd requirements (and steady state influx of Cd with
421 respect to PO₄³⁻) with increasing temperature and irradiance; in contrast, cultures of
422 cyanobacteria show a reduction in Cd uptake under similar conditions (Finkel et al.,
423 2007). However, in this case although there is a change in cell size, there does not
424 appear to be a major shift in the phytoplankton divisions throughout the summer with
425 more than 55% of the population comprising diatoms. Preliminary population

426 analyses indicate there is a shift away from large centrics in the early summer towards
427 smaller diatom species in the later bloom (Annett, pers. com.). In other words, these
428 results show that a switch does not have to be between phytoplankton divisions during
429 the bloom (e.g. diatoms to flagellates) in order to
430 influence the seawater Cd/PO₄³⁻ ratio but may be between phytoplankton genera
431 within a division.

432 The variation in Cd requirements with respect to macronutrients with population and
433 size structure in seawater may also influence the “global relationship” between Cd
434 and PO₄³⁻. For example, high nutrient upwelling zones favour the growth of
435 microplankton (in particular diatoms) with high Cd requirements. Temperate open
436 ocean regions favour the growth of other larger phytoplankton. Conversely, tropical
437 oligotrophic gyres favour the growth of picoplankton and autotrophic bacteria with
438 lower Cd requirements. Further, there is an effective microbial loop in these regions
439 that results in more rapid regeneration, which may mask the effect of biological
440 fractionation (Alvain et al., 2005; Follows et al., 2007).

441

442 ***4.3 Implications for glacial-interglacial reconstructions***

443

444 We have shown the non-linear relationship between Cd and PO₄³⁻ in seawater can be
445 explained by a combination of 1) water mass mixing; 2) differential biological
446 fractionation due to variation in micronutrient concentration, and 3) changes in
447 phytoplankton community structure. These processes are likely to change on glacial-
448 interglacial timescales, due to shifts in deep water formation processes and
449 atmospheric inputs, resulting in long-term changes in the Cd/PO₄³⁻ ratio of Southern
450 Ocean seawater.

451

452 *1) Deep water formation processes*

453 Currently, Atlantic Sector Southern Ocean deep water originates in the southern
454 region of the Weddell Sea near the continental shelf. Hence, these waters are replete
455 in micronutrients and Cd utilisation is lower than open ocean conditions, which results
456 in a relatively high seawater Cd/PO₄³⁻. However, benthic foraminifera stable isotopes
457 have been used to infer a shift in the deep convection site during the last glaciation to
458 the northern rim of the Weddell Sea because the ice sheet was pinned to the edge of
459 the continental shelf (Mackensen et al., 1996; Mackensen et al., 2001). Consequently,
460 the site of deep water formation may have had lower inputs of micronutrients and,
461 thus, surface waters may have experienced higher Cd utilisation and a lower seawater
462 Cd/PO₄³⁻. Such a shift in deep water convection could have lowered the Cd inventory
463 of Southern Atlantic deep waters, explaining, in part, the conflict between
464 foraminiferal δ¹³C and Cd/Ca data from the Southern Ocean LGM (Mackensen, 2001
465 and references therein).

466

467 *2) Atmospheric inputs*

468 A range of ice-core, terrestrial and marine records indicate an increase in dust supply
469 to the Southern Ocean during the last glaciation (Kohfeld and Harrison, 2001; Petit,
470 1999). Although the link between biological productivity and atmospheric supply of
471 micronutrients is poorly constrained and somewhat controversial (e.g. Maher and
472 Dennis, 2001), it is possible that phytoplankton may have experienced Fe and Zn
473 replete conditions in the Southern Ocean during the Last Glacial Maximum (LGM).
474 Indeed, one model suggests that, although global dust deposition may not have
475 increased dramatically, hydrological factors amplify the sensitivity of high latitude

476 regions to dust input resulting in over an order of magnitude enhancement in Fe
477 supply (Ridgwell and Watson, 2002). This would suggest growth conditions in the
478 LGM open Southern Ocean could have been analogous to the modern coastal system,
479 with lower Cd fractionation with respect to PO_4^{3-} .

480

481 3) *Phytoplankton community structure*

482 Changes in ocean stratification and sea-ice cover can shift phytoplankton community
483 structure (Abelmann et al., 2006; Arrigo, 1999) and, thus, changes in macro- and
484 micronutrient requirements (Arrigo, 2005). However, lack of constraint on
485 phytoplankton community structures over longer timescales further compounds the
486 ability to reconstruct past ocean nutrient budgets.

487

488 Shifts in the preformed $\text{Cd}/\text{PO}_4^{3-}$ ratio of seawater, and changes in biological
489 fractionation in Southern Ocean surface waters, could have significantly altered the
490 relationship between Cd/Ca recorded in foraminiferal calcite and ambient phosphate
491 concentrations. For example, Cd/Ca foraminiferal records have previously been
492 interpreted as showing no change in PO_4^{3-} utilisation in the Subantarctic, and a lower
493 PO_4^{3-} utilisation (5%) in the Antarctic during the LGM compared to today (35%;
494 Elderfield & Rickaby, 2000). However, assuming that the open Southern Ocean at
495 the LGM exhibited $\text{Cd}/\text{PO}_4^{3-}$ characteristics of modern coastal regions due to
496 enhanced atmospheric input, the same records imply PO_4^{3-} utilisation was higher in
497 the LGM Subantarctic compared to today. Further, a similar calculation suggests
498 PO_4^{3-} utilisation in the Antarctic Zone was lower than today (approximately 20%) but
499 declined less than previously calculated.

500

501 **5 Summary and conclusions**

502

503 We present a time series of Cd and macronutrient data from a coastal site adjacent to
504 the West Antarctic Peninsula, which shows that Cd is taken up during periods of high
505 biological productivity despite nearshore, micronutrient replete conditions. These
506 Antarctic coastal waters show high Cd/PO₄³⁻ and can impact the preformed nutrient
507 content of seawater in the open Southern Ocean through deep water formation and
508 mixing with water masses originating further north. We have demonstrated that the
509 non-linear relationship between Cd and PO₄³⁻ in seawater can be explained by a
510 combination of 1) water mass mixing; 2) differential biological fractionation due to
511 variation in micronutrient concentration, and 3) changes in phytoplankton community
512 structure, which can vary within a season. These processes are likely to change on
513 glacial-interglacial timescales, due to shifts in deep water formation processes and
514 atmospheric inputs, resulting in long-term changes in the Cd/PO₄³⁻ ratio of Southern
515 Ocean seawater. An understanding these shifts in the preformed Cd/PO₄³⁻ ratio of
516 seawater, and changes in biological fractionation in Southern Ocean surface waters,
517 could resolve discrepancies between benthic foraminiferal Cd/Ca records and other
518 paleonutrient proxies.

519

520 Acknowledgements:

521 The authors would like to thank the following: Sonja Ripperger for the use of the calibrated Cd isotope
522 spike; Samia Mantoura for help with silicic acid analysis; Amber Annett (University of Edinburgh) for
523 population analysis data; Damien Carson (University of Edinburgh), Chris Measures (University of
524 Hawaii) for useful discussion; John Arden for additional help on the ICP-MS; Andrew Clarke (British
525 Antarctic Survey) for biological and physical oceanographic data; the Bonner Laboratory marine
526 assistants Andrew Miller, Paul Mann and Helen Rossetti for collection of samples; the base
527 commander and staff of Rothera Research Station, British Antarctic Survey; and two anonymous
528 reviewers for insightful comments. The work was funded as part of NERC Antarctic Funding Initiative
529 AFI4-02. KRH is funded by NERC grant NER/S/A/2004/12390.

530

531 Abelman, A., Gersonde, R., Cortese, G., Kuhn, G. and Smetacek, V., 2006.
532 Extensive phytoplankton blooms in the Atlantic sector of the glacial Southern
533 Ocean. *Paleoceanography*, 21: doi:10.1029/2005PA001199.

534 Abollino, O., Aceto, M., Sacchero, G., Sarzanini, C. and Mentasti, E., 1995.
535 Determination of copper, cadmium, iron, manganese, nickel and zinc in
536 Antarctic sea water. Comparison of electrochemical and spectroscopic
537 procedures. *Analytica Chimica Acta*, 305: 200-206.

538 Adkins, J.F., McIntyre, K. and Schrag, D.P., 2002. The salinity, temperature, and
539 delta O-18 of the glacial deep ocean. *Science*, 298: 1769-1773.

540 Alvain, S., Moulin, C., Dandonneau, Y. and Bréon, F.M., 2005. Remote sensing of
541 phytoplankton groups in case 1 waters from global SeaWiFS imagery. *Deep-
542 Sea Research I*, 52: 1989-2004.

543 Álvarez, M., Rios, A.F. and Rosón, G., 2002. Spatio-temporal variability of air-sea
544 fluxes of carbon dioxide and oxygen in the Bransfield and Gerlache Straits
545 during Austral summer 1995-96. *Deep-Sea Research II*, 49: 643-662.

546 Armbrust, E.V., 2004. The genome of the diatom *Thalassiosira pseudonana*: ecology,
547 evolution and metabolism. *Science*, 306: 79-86.

548 Arrigo, K., 1999. Phytoplankton community structure and the drawdown of nutrients
549 and CO₂ in the Southern Ocean. *Science*, 283: 365-367.

550 Arrigo, K., 2005. Marine microorganisms and global nutrient cycles. *Nature*, 437:
551 349-355.

552 Asknes, D.L. and Egge, J.K., 1991. A theoretical model for nutrient uptake in
553 phytoplankton. *Marine Ecology Progress Series*, 70: 65-72.

554 Bakker, D.C.E., De Baar, H.J.W. and Bathmann, U.V., 1997. Changes of carbon
555 dioxide in surface waters during spring in the Southern Ocean. *Deep-Sea
556 Research II*, 44: 91-127.

557 Boyle, E.A., 1986. Paired carbon isotope and cadmium data from benthic
558 foraminifera: implications for changes in oceanic phosphorus, oceanic
559 circulation, and atmospheric carbon dioxide. *Geochimica et Cosmochimica
560 Acta*, 50: 265-276.

561 Boyle, E.A., 1988. Cadmium: chemical tracer of deep water paleoceanography,
562 *Paleoceanography*, 3: 471-489.

563 Clarke, A., Meredith, M.P., Wallace, M.I., Brandon, M.A. and Thomas, D.N., 2008.
564 Seasonal and interannual variability in temperature, chlorophyll and
565 macronutrients in Ryder Bay, northern Marguerite Bay, Antarctica. *Deep-Sea
566 Research II (Palmer LTER Special Issue)*.

567 Cullen, J.T., 2006. On the nonlinear relationship between dissolved cadmium and
568 phosphate in the modern global ocean: could chronic iron limitation of
569 phytoplankton cause the kink? *Limnology and Oceanography*, 51: 1369-1380.

570 Cullen, J.T., Chase, Z., Coale, K.H., Fitzwater, S.E. and Sherrell, R.M., 2003. Effect
571 of iron limitation on the cadmium to phosphorus ratio of natural
572 phytoplankton assemblages in the Southern Ocean. *Limnology and
573 Oceanography*, 48: 1079-1087.

574 Cullen, J.T. and Sherrell, R.M., 2005. Effects of dissolved carbon dioxide, zinc, and
575 manganese on the cadmium to phosphorus ratio in natural phytoplankton
576 assemblages. *Limnology & Oceanography*, 50: 1193-1204.

577 de Baar, H.J.W. and al, e., 1994. Cadmium versus phosphate in the world ocean.
578 *Marine Chemistry*, 46: 261-281.

579 Elderfield, H. and Rickaby, R., 2000. Oceanic Cd/P ratio and nutrient utilization in the
580 glacial Southern Ocean. *Nature*, 405: 305-310.

581 Finkel, Z.V., Quigg, A.S., Chiampia, R.K., Schofield, O.E. and Falkowski, P.G.,
582 2007. Phylogenetic diversity in cadmium:phosphorus ratio regulation by
583 marine phytoplankton. *Limnology & Oceanography*, 52: 1131-1138.

584 Follows, M.J., Dutkiewicz, S., Grant, S. and Chisholm, S.W., 2007. Emergent
585 biogeography of microbial communities in a model ocean. *Science*, 315: 1834-
586 1846.

587 Frew, R.D., 1995. Antarctic Bottom Water formation and the global cadmium to
588 phosphorous relationship. *Geophysical Research Letters*, 22: 2349-2352.

589 Frew, R.D., Heywood, K.J. and Dennis, P.F., 1995. Oxygen isotope study of water
590 masses in the Princess Elizabeth Trough, Antarctica. *Marine Chemistry*, 49:
591 141-153.

592 Frew, R.D. and Hunter, K.A., 1992. Influence of Southern Ocean waters on the
593 cadmium-phosphate properties of the global ocean. *Nature*, 360: 144-146.

594 Gibson, J.A.E. and Trull, T.W., 1999. Annual cycle of fCO₂ under sea-ice and in open
595 water in Prydz Bay, East Antarctica. *Marine Chemistry*, 66: 187-200.

596 Gligora, M., Plenkovic-Moraj, A., Kralj, K., Grigorszky, I. and Peros-Pucar, D., 2007.
597 The relationship between phytoplankton species dominance and environmental
598 variables in a shallow lake (Lake Vrana, Croatia). *Hydrobiologia*, 584: 337-
599 346.

600 Gobeil, C., Macdonald, R.W. and Sundby, B., 1997. Diagenetic separation of
601 cadmium and manganese in suboxic continental margin sediments.
602 *Geochimica Cosmochimica Acta*, 61: 4647-4654.

603 Ho, T.Y. et al., 2003. The elemental composition of some marine phytoplankton.
604 *Journal of Phycology*, 39: 1145-1159.

605 Hoppema, M., Stoll, M.H.C. and De Baar, H.J.W., 2000. CO₂ in the Weddell Gye and
606 Antarctic Circumpolar Current: austral autumn and early winter. *Marine
607 Chemistry*, 72: 203-220.

608 Hunter, K.A. and Boyd, P.W., 1997. Has trace metal marine biogeochemistry finally
609 come of age? In: R.B. Macaskill (Editor), *Proceedings of the Trace Element
610 Group of New Zealand*. Waikato University, Waikato.

611 Jones, C.J. and Murray, J.W., 1984. Nickel, cadmium and copper in the northeast
612 Pacific off the coast of Washington. *Limnology and Oceanography*, 29: 711-
613 720.

614 Kirkwood, D.S., 1996. Nutrients: practical notes on their determination in seawater.
615 *ICES Techniques in Marine Environmental Sciences*, no. 17. International
616 Council for the Exploration of the Seas, Copenhagen, 23 pp.

617 Kohfeld, K.E. and Harrison, S.P., 2001. DIRTMAP: the geological record of dust.
618 *Earth Science Reviews*, 54: 81-114.

619 Lacan, F., Francois, R., Yongcheng, J. and Sherrell, R.M., 2006. Cadmium isotopic
620 composition in the ocean. *Geochimica Cosmochimica Acta*, 70: 5104-5118.

621 Lane, T.W. and Morel, F.M.M., 2000. Regulation of carbonic anhydrase expression
622 by zinc, cobalt and carbon dioxide in the marine diatom *Thalassiosira
623 weissflogii*. *Plant Physiology*, 123: 345-352.

624 Lane, T.W. et al., 2005. A cadmium enzyme from a marine diatom. *Nature*, 435: 42.

625 Lee, J.G., Ahner, B.A. and Morel, F.M.M., 1996. Export of cadmium and
626 phytochelatin by the marine diatom *Thalassiosira weissflogii*. *Environ. Sci.
627 Technol.*, 30: 1814-1821.

628 Lee, J.G. and Morel, F.M.M., 1995. Replacement of zinc by cadmium in marine
629 phytoplankton. *Marine Ecology Progress Series*, 127: 305-309.

630 Löscher, B.M., de Baar, H.J.W., de Jong, E., Veth, C. and Dehairs, F., 1997. The
631 distribution of Fe in the Antarctic Circumpolar Current. *Deep-Sea Research II*,
632 44: 143-188.

633 Löscher, B.M., de Jong, J.T.M. and de Baar, H.J.W., 1998. The distribution and
634 preferential biological uptake of cadmium at 6 degrees W in the Southern
635 Ocean. *Marine Chemistry*, 62: 259-286.

636 Mackensen, A., 2001. Oxygen and carbon stable isotope traces of Weddell Sea water
637 masses: new data and some paleoceanographic implications. *Deep-Sea*
638 *Research I*, 48: 1401-1422.

639 Mackensen, A., Hubberten, H.-W., Scheele, N. and Schlitzer, R., 1996. Decoupling of
640 $\delta^{13}\text{C}_{\Sigma\text{CO}_2}$ and phosphate in Recent Weddell Sea deep and bottom water:
641 implications for glacial Southern Ocean paleoceanography. *Paleoceanography*,
642 11: 203-215.

643 Mackensen, A., Rudolph, M. and Kuhn, G., 2001. Late Pleistocene deep-water
644 circulation in the subantarctic eastern Atlantic. *Global and Planetary Change*,
645 30: 197-229.

646 Maher, B.A. and Dennis, P.F., 2001. Evidence against dust-mediated control of
647 glacial-interglacial changes in atmospheric CO_2 . *Nature*, 411: 176-180.

648 Martin, J.H., Gordon, R.M. and Fitzwater, S.E., 1990. Iron in Antarctic waters.
649 *Nature*, 345: 156-158.

650 Martin, J.H., Knauer, G.A., Karl, D.M. and Broenkow, W.W., 1987. VERTEX -
651 carbon cycling in the Northeast Pacific. *Deep-Sea Research Oceanogr. Part A*,
652 34: 267-285.

653 Meredith, M.P. et al., 2008. Variability in the freshwater balance of northern
654 Marguerite Bay, Antarctic Peninsula: results from $\delta^{18}\text{O}$. *Deep-Sea Research*,
655 *SO-GLOBEC Special Issue*.

656 Meredith, M.P., Renfrew, I.A., Clarke, A., King, J.C. and Brandon, M.A., 2004.
657 Impact of the 1997/1998 ENSO on upper ocean characteristics in Marguerite
658 Bay, western Antarctic Peninsula. *Journal of Geophysical Research*, 109:
659 doi:10.1029/2003JC001784.

660 Morel, F.M.M. and Price, N.M., 2003. The biogeochemical cycles of trace metals in
661 the oceans. *Science*, 300: 944-947.

662 Morel, F.M.M. et al., 1994. Zinc and carbon co-limitation of marine phytoplankton.
663 *Nature*, 369: 740-742.

664 Nolting, R.F., Ramkema, A. and Everaarts, J.M., 1999. The geochemistry of Cu, Cd,
665 Zn, Ni and Pb in sediment cores from the continental slope of the Banc
666 d'Argiun (Mauritania). *Continental Shelf Research*, 19: 665-691.

667 Park, H., Song, B. and Morel, F.M.M., 2007. Diversity of the cadmium-containing
668 carbonic anhydrase in marine diatoms and natural waters. *Environmental*
669 *Microbiology*, 9: 403-413.

670 Petit, J.R., 1999. Climate and atmospheric history of the past 420 000 years from the
671 Vostok ice core, Antarctica. *Nature*, 399: 429-436.

672 Prendez, M. and Carrasco, M.A., 2003. Elemental composition of surface waters in
673 the Antarctic Peninsula and interactions with the environment. *Environmental*
674 *Geochemistry and Health*, 25: 347-363.

675 Prendez, M., Munoz, V., Villanueva, V., Montero, J.C. and Godoy, J., 1996. Estudio
676 quimico de las aguas continentales de peninsula Fildes, isla Rey Jorge,
677 Antarctica. *Serie Cientifica INACH*, 46: 9-29.

678 Price, N.M. and Morel, F.M.M., 1990. Cadmium and cobalt substitution for zinc in a
679 marine diatom. *Nature*, 344: 658-660.

- 680 Ridgwell, A.J. and Watson, A., 2002. Feedback between aeolian dust, climate, and
681 atmospheric CO₂ in glacial time. *Paleoceanography*, 17: 1059.
- 682 Ripperger, S. and Rehkämper, M., 2007a. A highly sensitive MC-ICPMS method for
683 Cd/Ca analyses of foraminiferal tests. *Journal of Analytical Atomic*
684 *Spectrometry*, 22: 1275-1283.
- 685 Ripperger, S. and Rehkämper, M., 2007b. Precise determination of cadmium isotope
686 fractionation in seawater by double spike MC-ICPMS. *Geochimica*
687 *Cosmochimica Acta*, 71: 631-642.
- 688 Ripperger, S., Rehkämper, M., Porcelli, D. and Halliday, A.N., 2007. Cadmium
689 isotope fractionation in seawater - A signature of biological activity. *EPSL*,
690 261: 670-684.
- 691 Sañudo-Wilhelmy, S.A., Olsen, K.A., Scelfo, J.M., Foster, T.D. and Flegal, A.R.,
692 2002. Trace metal distributions off the Antarctic Peninsula in the Weddell Sea.
693 *Marine Chemistry*, 77: 157-170.
- 694 Smith, D.A., Hofmann, E.E., Klinck, J.M. and Lascara, C.M., 1999. Hydrography and
695 circulation of the West Antarctic Peninsula continental shelf. *Deep-Sea*
696 *Research I*, 46: 925-949.
- 697 Sunda, W.G. and Huntsman, S.A., 1998. Control of Cd concentrations in a coastal
698 diatom by interactions among free ionic Cd, Zn and Mn in seawater. *Environ.*
699 *Sci. Technol.*, 32: 2961-2968.
- 700 Takahashi, T. et al., 2002. Global sea-air CO₂ flux based on climatological surface
701 ocean pCO₂, and seasonal biological and temperature effects. *Deep-Sea*
702 *Research II*, 49: 1601-1622.
- 703 Van Geen, A. and Luoma, S.N., 1993. Trace metals (Cd, Cu, Ni and Zn) and nutrients
704 in coastal waters adjacent to San Francisco Bay, California. *Estuaries*, 16: 559-
705 566.
- 706 Wang, W. and Dei, R., 2001. Effects of major nutrient additions on metal uptake in
707 phytoplankton. *Environmental Pollution*, 111: 233-240.
- 708 Wen, Y.-H., Vezona, A. and Peters, R.H., 1997. Allometric scaling of compartmental
709 fluxes of phosphorus in freshwater algae. *Limnology and Oceanography*, 42:
710 45-56.
- 711 Westerlund, S. and Ohman, P., 1991. Cadmium, copper, cobalt, nickel, lead and zinc
712 in water column at Weddell Sea, Antarctica. *Geochimica Cosmochimica Acta*,
713 55: 2127-2146.
- 714 Wu, J. and Boyle, E.A., 1997. Low blank preconcentration technique for the
715 determination of lead, copper, and cadmium in small-volume seawater
716 samples by isotope dilution ICPMS. *Analytical Chemistry*, 69: 2464-2470.
- 717 Xu, Y., Feng, L., Jeffrey, P.D., Shi, Y. and Morel, F.M.M., 2008. Structure and metal
718 exchange in the cadmium carbonic anhydrase of marine diatoms. *Nature*, 452:
719 56-61.
- 720 Yeats, P.A., 1998. An isopycnal analysis of cadmium distribution in the Atlantic
721 Ocean. *Marine Chemistry*, 61: 15-23.
- 722
- 723

724 Figure 1: All seawater dissolved Cd and Dissolved Inorganic Phosphate (DIP) data for the
725 global ocean (surface and deep waters in open symbols) for different ocean basins (Boyle et
726 al., 1976; Bruland, 1980; Bruland & Franks, 1983; Danielsson et al., 1985; Sakamoto-Arnold
727 et al., 1987; Hunter & Ho, 1991; Nolting & de Baar, 1994; Löscher et al., 1998; Fitzwater et
728 al., 2000; Abe, 2001, 2002; Ellwood, 2004). Also included are data from semi-enclosed
729 South China Sea (Chen et al., 2005). Deep water data shown in closed symbols from de Baar
730 et al., (1994).

731

732 Figure 2: Map of study site off the West Antarctic Peninsula, with the RaTS site shown by the
733 grey box.

734

735 Figure 3: External reproducibility of 1 ppb Alfa Zürich standard and in-house standard
736 (“Ryder06”) using A) $^{110}\text{Cd}/^{111}\text{Cd}$ and B) $^{110}\text{Cd}/^{114}\text{Cd}$. Error bars show internal precision
737 ($\pm 1.3\%$).

738

739 Figure 4: Comparison of methods for the analysis of dissolved Cd in seawater samples of
740 using two different isotope ratios for isotope dilution ($\pm 1\sigma$).

741

742

743 Figure 5: Pigment and nutrient concentrations from 15 m collected at the RaTS site from
744 2005-2006. A) Total chlorophyll *a* concentrations (grey square; B) size fractionated chl *a*
745 (data courtesy of BAS); macronutrient concentrations C) nitrate (white triangles), D) silicic
746 acid (black squares) and E) phosphate (white diamonds); micronutrient concentrations F)
747 cadmium (measured by standard addition (SA; grey dots) and isotope dilution (ID; black
748 circles) and G) $\text{Cd}/\text{PO}_4^{3-}$. (grey circles). N and P measurements carried out by Weston, UEA,
749 and Carson, Edinburgh. All errors bars show $\pm 2\sigma$.

750

751

752

753 Figure 6: Fractionation of dissolved Cd and PO_4^{3-} or DIP in Southern Ocean waters.
754 Upwelling CDW (cyan dashed line) is formed from a mixture of NADW and AABW.
755 Endmember compositions shown in the large cyan circles (de Baar and al, 1994; Elderfield
756 and Rickaby, 2000; Frew, 1995; Westerlund and Ohman, 1991). The mixing of these water
757 masses can be observed in measurements of Cd and P measurements in Subantarctic Zone
758 Waters (SAW, black circles), Polar Front regions (PF, red circles) and Antarctic Zone Waters
759 (AAW, green circles). In open water regions (e.g. Subantarctic Zone, black circles),
760 fractionation of Cd with respect to P follows a simple fractionation trend given by Equation 6
761 with a constant fractionation factor, $\alpha_{\text{Cd-P}} = 3.5$. In coastal conditions in the (CCSW e.g. this
762 study, dark blue circles and the Princess Elizabeth Trough, PET, yellow circles) there is 1)
763 stock of Cd, Cd_{xs} , that is not utilised (Equation 7), and 2) a lower fractionation factor, $\alpha_{\text{Cd-P}} =$
764 2.0. Utilisation and decay of nutrients follow trajectories given by the grey arrows. Note that
765 the $\text{Cd}/\text{PO}_4^{3-}$ of upwelling waters will depend on the depth of mixing due to the deeper
766 regeneration cycle of Cd.

767

768

Standard	Quoted concentration (ppb)	Measured concentration
IAPSO K15	0.08-0.12	0.087 ± 0.010
NASS-5	*0.023 ± 0.003	0.024 ± 0.004

769

*Certified seawater reference material for trace metals, National Research Council Canada

770

Table 1: Cd analysis of reference seawater standards. Errors are ±2σ.

771

772

Solution	¹¹⁰ Cd/ ¹¹¹ Cd	¹¹⁰ Cd/ ¹¹⁴ Cd
Alfa Cd Zürich (lot 901463E)	0.977047 (50)	0.438564 (50)
Spike	72.7346 (5072)	79.4532 (5540)

773

Table 2: Isotope ratios of standards (Ripperger and Rehkämper, 2007b). Uncertainties in

774

brackets denote 2σ.

775

776

Instrument	Thermo Finnigan Element2 magnetic sector ICP-MS with Cetac ASX-100 autosampler
Isotopes measured	95, 98, 106, 110, 111, 112, 114, 118, all in Low Resolution mode
Scan parameters	mass window 5%, 400 samples/peak, segment duration 40 ms
E-Scan range	30%
Analysis time	4.00 min (10 runs × 73 passes)
Plasma power	1450 W
Sample gas	1.12 L/m
Sample uptake rate	ca. 100 µL/min

777

Table 3: Analytical parameters of ICP-MS analysis

778

779

Isotope	% Abundance (natural)	Interferences	% signal
¹⁰⁶ Cd	1.25	¹⁰⁶ Pd	68
¹¹⁰ Cd	12.49	¹¹⁰ Pd, ⁹⁴ MoO ⁺	6, 2
¹¹¹ Cd	12.80	⁹⁵ MoO ⁺	12
¹¹² Cd	24.13	¹¹² Sn, ⁹⁶ MoO ⁺	3, 7
¹¹⁴ Cd	28.73	¹¹⁴ Sn, ⁹⁸ MoO ⁺	2, 8

780

Table 4: Interferences on isotopes of cadmium, and mean percentage of the signal of each

781

interference. The percent signal calculated as follows, and averaged for all samples

782

measured:

783

784

% signal = (counts from interference at mass peak)/(total counts at mass peak) x 100.

785

786

787

788

789

790

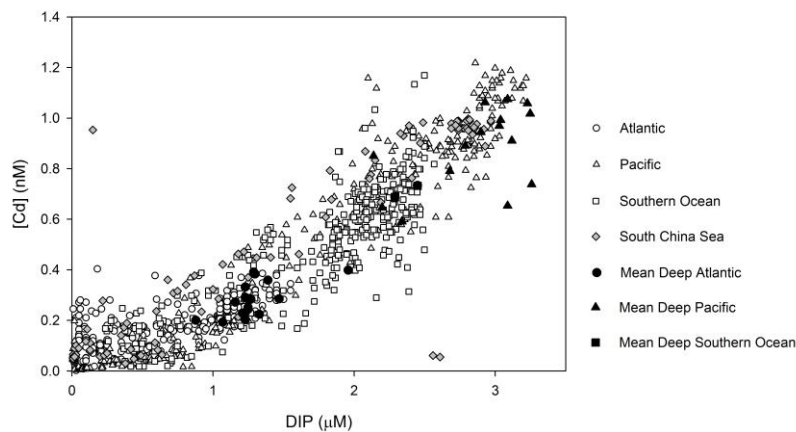
791

792

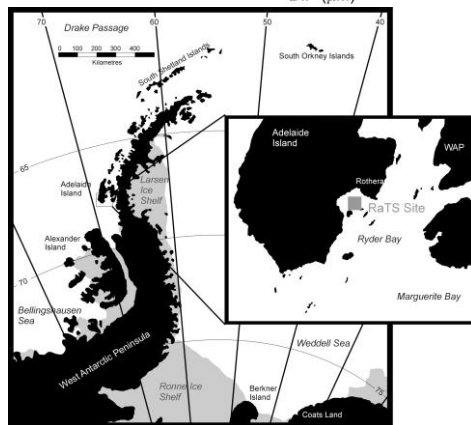
793

Region	[Fe] (nM)	[Zn] (nM)	Reference
Palmer Station, WAP	4-6	4-5	(Sañudo-Wilhelmy et al., 2002)
King George Island, South Georgia		> 40	(Prendez and Carrasco, 2003; Prendez et al., 1996)
Weddell Sea	1-6	3-5	(Westerlund and Ohman, 1991)
Terra Nova Bay, Antarctica	3.5	5	(Sañudo-Wilhelmy et al., 2002)
Open Southern Ocean	0.2-0.5	0.2-0.5	(Abollino et al., 1995; Löscher et al., 1997; Löscher et al., 1998; Martin et al., 1990)

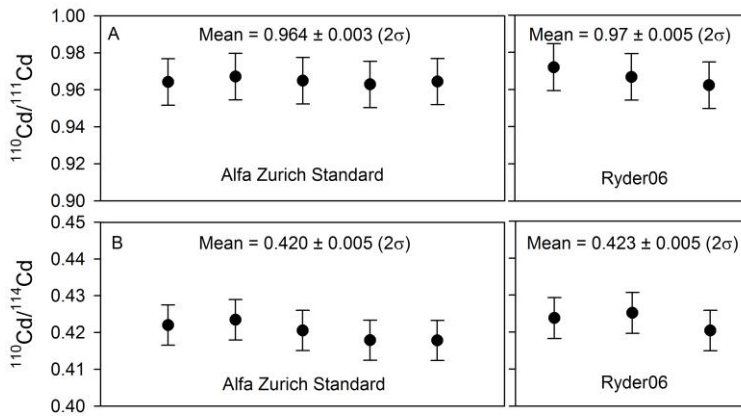
794 Table 5: Fe and Zn concentrations of some regions in the Southern Ocean and coastal
795 Antarctica.
796
797
798



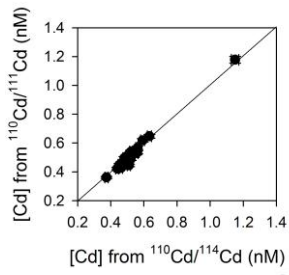
799



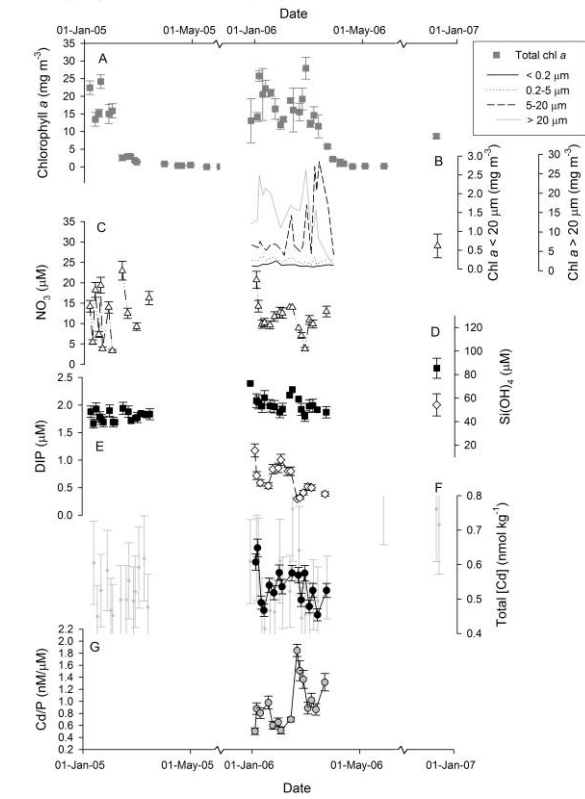
800



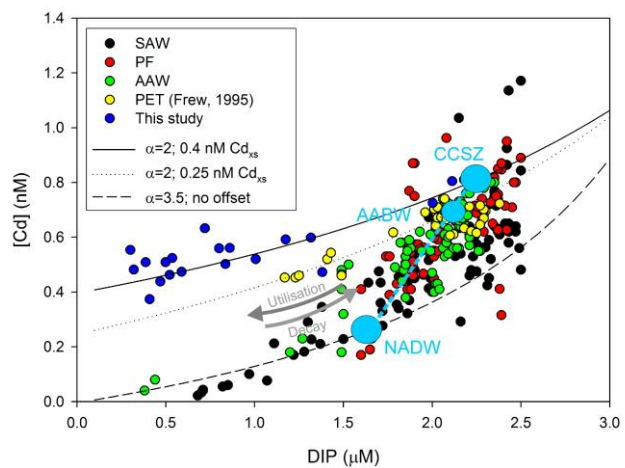
801



802



803



804